School of Information Technology and
Engineering at the ADA University

School of Engineering and Applied Science
at the George Washington University

DESIGN AND SIMULATION OF A 25MW SOLAR POWER PLANT IN BAKU CITY

A Thesis
Presented to the Graduate Program of Electrical and Power Engineering
of the School of Information Technology and Engineering
ADA University

In Partial Fulfillment
of the Requirements for the Degree
Master of Science in Electrical and Power Engineering
ADA University

By
Guliyev Ilgar

December, 2023

THESIS ACCEPTANCE

This Thesis by: [Guliyev Ilgar]

Entitled: *Design and Simulation of a 25MW Solar Power Plant in Baku City*

has been approved as meeting the requirement for the Degree of Master of Science in Electrical and Power Engineering of the School of Information Technology and Engineering, ADA University.

Approved:

Orkhan Karimzade	
(Adviser)	(Date)
Wisam Al Dayyeni	
(Program Director)	(Date)
Abzatdin Adamov	
(Dean)	(Date)

ACADEMIC INTEGRITY STATEMENT

"I affirm that this is my own work, I attributed where I used the work of others, I did not facilitate academic dishonesty for myself or others, and I used only authorized resources for my Thesis, per the ADA University Academic Integrity requirements. If I failed to comply with this statement, I understand consequences will follow my actions. Consequences may range from failing the course to expulsion from the program/university and may include a transcript notation."

Guliyev Ilgar		24.12.2023
(Full Name)	(Signature)	(Date)

ABSTRACT

Recent advancements in technology have facilitated the development of power generation systems that harness solar energy through the utilization of floating photovoltaic (FPV) systems. The utilization of floating photovoltaic systems is both a new and prevalent technique for incorporating PV modules within water frameworks, thus preserving land area. Additionally, the electrical efficiency of a solar system exhibits a decline as the temperature rises. Thus, in order to enhance efficiency, it is necessary to cool the photovoltaic (PV) module by implementing a heat removal mechanism. The water below naturally cools FPV projects, providing them with an advantage. This study explores the feasibility of implementing floating solar panels in Boyukshor Lake, located in Baku City. The proposed power plant is a grid-tied system with a capacity of 25 MW. The site exhibits convenient accessibility and adequate water depth, which ranges between 3.40 meters and 4.20 meters. The FPV energy project in Boyukshor Lake involves the assessment of several factors, such as panel positioning, solar panel efficiency, and surface area availability. The construction of the single line diagram is determined by considering the solar module and inverter as independent variables. The investigation selected two types of PV modules and string inverters based on their parameters. The analysis demonstrated the mean global horizontal irradiance (GHI) for the specified region is 1523.4 kilowatt-hours per square meter per year. The master thesis consists of three simulations. In the first and second cases, the chosen arrangement of components for the floating solar power plant comprises 45791 panels with a total power output of 29764 kW. The panels are organized into 29 series and accompanied by 1579 string solar panels. The first and second cases include a 3125 kW inverter, while the third case will be simulated with a 100 kW inverter. In the simulation, both AC and DC

cables are utilized. The design exhibits anticipated system performance metrics, including a performance ratio, system efficiency, and capacity factor. Also, this study provides an economic and environmental evaluation of the above-mentioned simulations. These considerations contribute to the development of a complete model that accurately predicts the entire electricity generation of the Boyukshor floating PV power plant. As a result, this method of producing electricity involves analyzing simulated data, looking at the theoretical underpinnings, evaluating the capital investment, operational costs, and maintenance costs, as well as assessing its numerous advantages.

Contents

LIST OF FIGURES

LIST OF TABLES

LIST OF ABBREVIATIONS

Abbreviation	Explanation
FPV	Floating Photovoltaic
PV	Photovoltaic
GHI(GlobHor)	Global Horizontal Irradiance
DC	Direct Current
AC	Alternating Current
O&M	Operation and Maintenance
PR	Performance Ratio
SPV	Solar Photovoltaic
TF	Transposition Factor
GlobInc	Global Incident Irradiance
GTI	Global Tilt Irradiance
TCF	Temperature Correction Factor
CF	Capacity Factor
SLD	Single Line Diagram
CAPEX	Capital Expenditure
OPEX	Operational Expenditure
LCOE	Levelized Cost of Energy
NPV	Net Present Value
IRR	Internal Rate of Return
ROI	Return on Investment
GHG	Greenhouse gases
LCE	Lifecycle Carbon Emission

CHAPTER ONE

1.1 INTRODUCTION

There exists a significant potential for the deployment of floating solar photovoltaic (PV) systems in Boyukshor Lake, as suggested in the research article. The objective of this master's thesis is to conduct an analysis of the power potential and site feasibility, as well as the layout of the floating photovoltaic (FPV) components. Additionally, the study intends to evaluate the system performance and economic analysis of a 25 MW solar plant achieved through the proposed design. In order to enhance the precision of the findings, the study will integrate mathematical computation techniques with optimization and simulation methodologies employing PVsyst software. In the proposed project, a portion equivalent to 0.8–0.88% of the total area of the Boyukshor lake will be utilized, depending on the configuration of the PV plant.

Climate conditions, operational electrical characteristics, and design parameters are just a few of the variables that affect photovoltaic module performance. These design parameters include the outside temperature, solar irradiation, module temperature, and combination of monocrystalline or polycrystalline panels with string inverters. The photovoltaic module commonly exhibits an efficiency range of 4–17% in converting solar energy into electrical power, with the specific value dependent on the characteristics. The elevated level of solar radiation intensifies the temperature of the module, concurrently diminishing the efficiency of the photovoltaic cell. The direct current (DC) output generated by photovoltaic (PV) systems is transformed into alternating current (AC) through the utilization of an inverter [1]. The key elements of the photovoltaic (PV) system consist of PV modules and inverters [2]. The identification of suitable locations and optimal photovoltaic

(PV) technologies is of great importance for the widespread implementation of large-scale solar photovoltaic systems [3]. The cited research articles provide a comprehensive overview of the development phase of FPV technology [4] and its subsequent evaluation of solar plants [5] [6] [7].

1.2 MOTIVATION

Fossil fuels such as gas and oil are utilized to enhance electricity generation. The persistent utilization of fossil fuels for electrical generation has led to the continuing depletion of conventional resources. The utilization of fossil fuels for power generation emits a significant amount of carbon dioxide into the environment. Solar and wind energy sources have the potential to serve as viable alternatives to conventional power plants [8]. The photovoltaic module is capable of converting photon energy into electrical energy in an environmentally friendly manner. The implementation of a floating solar PV plant in Boyukshor Lake is an excellent concept for harnessing solar energy. This approach effectively decreases environmental pollution, mitigates land shortages, and fulfills the growing energy demands of Azerbaijan [9].

1.3 THESIS STRUCTURE

This article presents a proposal for the construction of a floating solar power plant on Boyukshor Lake, located in Baku. Section II of the paper delves into the research methodology that covered data collection and its assessment. Additionally, theoretical knowledge is shown to have been used in simulation software. The site selection process is discussed in Section III. The results of the simulated data are discussed in Section IV. Section V is regarding the economic evaluation of the Boyukshor Solar Project. Finally, Section VI emerges the environmental contribution of this solar project. Case 3 simulation results will be shown in Section VII.

CHAPTER TWO

RESEARCH METHODOLOGY

2.1. DATA COLLECTION

The utilization of secondary data in this study substantiated the layout phase of the floating photovoltaic. The necessary information comprises the subsequent elements: the depth of the mentioned lake, the map of the lake and its associated features, solar radiation and meteorological conditions at the specific location, parameters for the components of the FPV plant, and additional related information.

2.2. AN EVALUATION OF DATA

Three analyses were conducted in this study, namely area feasibility assessment, system component layout evaluation, and efficiency analysis of the proposed floating photovoltaic plant.

- A study on the feasibility of the site: The feasibility evaluation was conducted by taking into account many factors, including the data on the geographical dimensions of the lake (such as area and depth) obtained from contour maps, as well as information on insolation, wind speed, temperature, and the accessibility of the site.
- The study focuses on the analysis of component configuration. The research was conducted by using two distinct categories of solar panels and string inverters as independent variables. Two FPV modules that have been chosen for analysis are the monocrystalline and polycrystalline panels. Monocrystalline panels that are simulated belong to the firm "ZN Shine Solar" (650 W, 32 V), whereas polycrystalline panels are manufactured by "Photo Watt" (650 W, 32 V). The solar panels under consideration possess a number of parameters, including P_{nom} (W), V_{mpp} (V), I_{mpp} (A), V_{oc} (V), I_{scr} (A), efficiency (%), T_{CF} (mA/^{o}C), and size (mm).

Table 2.1. Electrical data of a) ZN Shine Solar and b) Photo watt module

a)

Electrical data	Rated
Nominal Power (+/-3%)	650 W
Rated Voltage at Max. power (Vmpp)	37.7 V
Rated Current at Max. power (Impp)	17.25 A
Open-Circuit voltage (Voc)	45.2 V
Short circuit current (Iscr)	18.27 A
Panel efficiency (η)	0.2235 %
Temperature coefficient(T_{CF})	9.1 mA/°C

b)

Electrical data	Rated
Nominal Power (+/-3%)	650 W
Rated Voltage at Max. power (Vmpp)	37.90 V
Rated Current at Max. power (Impp)	17.16 A
Open-Circuit voltage (Voc)	45 V
Short circuit current (Iscr)	18.39 A
Panel efficiency (η)	22.35 %
Temperature coefficient(T_{CF})	9.2 mA/°C

The string inverters utilized in this study are the Sungrow (3125 kW, 875–1300 V) and Sepsa (100 kW, 450–820 V). The parameters under consideration for the inverter include the maximum input power ($P_{in,max}$) in kilowatts, the maximum output power ($P_{out,max}$) in kilowatts, the direct current voltage (V_{DC}) in volts, the maximum voltage at the maximum power point (V_{mp}) in volts, the maximum current at the maximum power point (I_{mp}) in amperes, the maximum direct current input ($I_{DC,max}$) in amperes, the number of maximum power point trackers (MPPT), the number of inputs, and the efficiency expressed as a percentage. For the next phase, a Sepsa inverter (100 kW) will be simulated with the solar panel with the highest efficiency. In addition to employing other components, control variables are utilized. The selection of control variables was determined by a thorough examination and comparison of parameters.

Table 2.2. Simulated cases.

Inverters / *PV Modules*	*Sungrow (3125 kW)*	*Sepsa (100kW)*
ZN shine Solar (650 W,32 V) – Monocrystalline module	Case 1	Case 3
Photo watt (650 W, 32 V) – Polycrystalline module	Case 2	

- The assessment of system performance focused on three key attributes: system efficiency, performance ratio (PR), and capacity factor (CF).

2.3. PARAMETERS AND COMPONENT INSIGHTS

The layout and efficiency parameters of the considered plant were determined using mathematical computations. This research utilizes a considerable number of equations. The process involves performing calculations on the variables listed below:

1. Global tilt irradiance refers to the quantification of solar radiation received on a surface that is inclined at an angle relative to the horizontal plane.

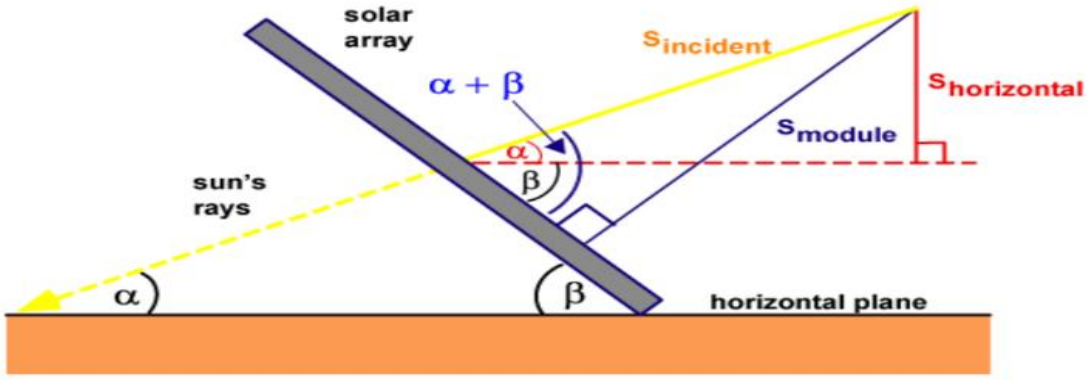

Figure 2.1. The diagram of Global Tilt Irradiance [10]

The amount of solar radiation received by a tilted panel surface is the component of incident solar radiation that is perpendicular to the module's surface. The provided diagram illustrates the methodology for determining the amount of radiation received by a tilted surface (S_{module}) based on either the solar radiation recorded on a horizontal plane (S_{horiz}), or the solar radiation measured perpendicular to the sun ($S_{incident}$) [11].

The equations that establish the relationship between S_{module}, S_{horiz}, and $S_{incident}$ are as follows:

$$S_{horizontal} = S_{incident} * \sin\alpha \quad (2.1)$$

$$S_{module} = S_{incident} * \sin(\alpha+\beta) \quad (2.2)$$

$$\alpha = 90 - \varphi + \delta \quad (2.3)$$

$$\delta = 23.45° \sin\left[\frac{360}{365}\right](284 + d) \quad (2.4)$$

The variable α represents the elevation angle, whereas the variable β denotes the tilt angle of the panel, measured with respect to the horizontal. Let "φ" represent the latitude, and "σ" denote the previously provided declination angle. Where "d" is the numerical value corresponding to a certain day within a given year. It should be noted that the expression (284+d) might be considered mathematically identical to the (d-81). By analyzing these equations, it is possible to establish a correlation between the variables S_{module} and S_{horiz}.

$$\text{Smodule} = \frac{\text{Shorizontal} * \sin(\alpha+\beta)}{\sin\alpha} \quad (2.5)$$

2. The Temperature Correction Factor (TCF) is a numerical value used to adjust for the effects of temperature on a particular measurement or calculation. Each photovoltaic module is assigned a temperature coefficient. The temperature coefficient quantifies the extent to which the panel's performance will degrade with a one-degree Celsius (°C) increase in temperature. Typically, panels exhibit a temperature coefficient ranging from -0.2% /°C to -0.5%/°C when subjected to conventional laboratory settings, with the ambient temperature maintained at 25°C. Solar panels with superior temperature resistance provide better efficiency. A panel's performance is enhanced as the temperature coefficient approaches zero. All solar panel manufacturers are obligated to provide an indication of the temperature coefficient value. [12]. It is

mandatory for all manufacturers of solar panels to indicate the temperature coefficient value.

3. The choice of solar panels has a significant role in the design of floating photovoltaic (FPV) systems. The selected solar panel types were monocrystalline and polycrystalline, each possessing distinct advantages and disadvantages in terms of efficiency, space use, cost, and temperature tolerance. As the Boyukshor FPV project had a fixed structure, every advantage of these types of panels is discussed below.

The primary distinction between these modules is in the level of crystal clarity shown by the panel cells. Photovoltaic cells in monocrystalline modules are made up of a single crystal of silicon. Solar cells in polycrystalline modules, on the other hand, are made up of many pieces of silicon that have been fused together. The level of cellular purity in monocrystalline solar modules is significantly greater than that observed in polycrystalline solar modules.

Table 2.3. The difference between monocrystalline and polycrystalline wafers [13]

Item	Monocrystalline wafer	Polycrystalline wafer
Microstructure	Ordered crystal structure	Combination of small crystal particles
Dislocation density（cm-2）	$< 10^3$	10^3~10^9
Iron impurity	Lower	Higher
Oxygen impurity	Higher	Lower
Macrostructure	Chamfer/No spots	No chamfer/Spots
Bending strength	Higher	Lower

Monocrystalline panels utilized in stationary photovoltaic (PV) systems exhibit enhanced efficiency, better space utilization, and better aesthetics but come at a higher cost. In contrast, polycrystalline panels exhibit cost-effectiveness, enhanced temperature tolerance, and moderate efficiency, although they require more space.

The selection between the two types of solar panels is contingent upon various aspects, including financial considerations, spatial limitations, and aesthetic inclinations. Monocrystalline panels are regarded as a high-end option, while polycrystalline panels provide a favorable combination of performance and cost-effectiveness. The following table 2.4 illustrates the distinction between the two varieties of solar modules.

Table 2.4. The difference between monocrystalline and polycrystalline cells [13]

Item	Monocrystalline cell	Polycrystalline cell
Appearance	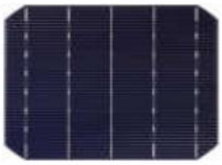	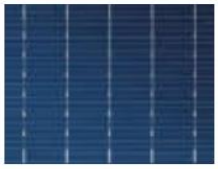
Chamfer	Yes	No
spots	No	Yes
Color	Darker	Light blue, blue, medium blue

The efficiency of a solar panel is determined by dividing the quantity of energy it collects by the quantity of energy it generates. An efficiency percent indicates that power is generated from that percent of the solar radiation, while the remaining solar radiation is converted to heat.

In contrast to polycrystalline solar panels, monocrystalline solar cells consist of a solitary crystal, which enhances their energy generation and spectral response. As a result, monocrystalline solar panels exhibit superior performance [14].

In practical terms, the efficiency range of monocrystalline solar modules spans from 16% to 25%, whereas that of polycrystalline solar modules falls within the range

of 14% to 23%. This implies that, when comparing solar panels on the same area, monocrystalline modules exhibit higher efficiency [15].

One notable benefit of monocrystalline PV modules is their superior cell crystal clarity, which enables an extended production duration compared to polycrystalline solar panels. In addition to its enhanced efficiency, this particular panel exhibits a prolonged duration of energy generation compared to polycrystalline PV modules.

4. A string inverter is interconnected with a series of solar panels, commonly referred to as the solar array. The solar panels are interconnected in a series configuration. Then, the n-number of strings is connected in parallel to the input of MPPT technology, as seen in Figure 2. Typically, each MPPT module connects to a range of 2-4 PV strings. The predetermined number of photovoltaic (PV) strings is initially connected within each maximum power point tracking (MPPT) module and regulated by the MPPT. After the regulation, the output voltage of MPPT modules will be the same. Finally, the inverter integrates the direct current obtained from each individual MPPT module and simultaneously inverts it into alternating current.

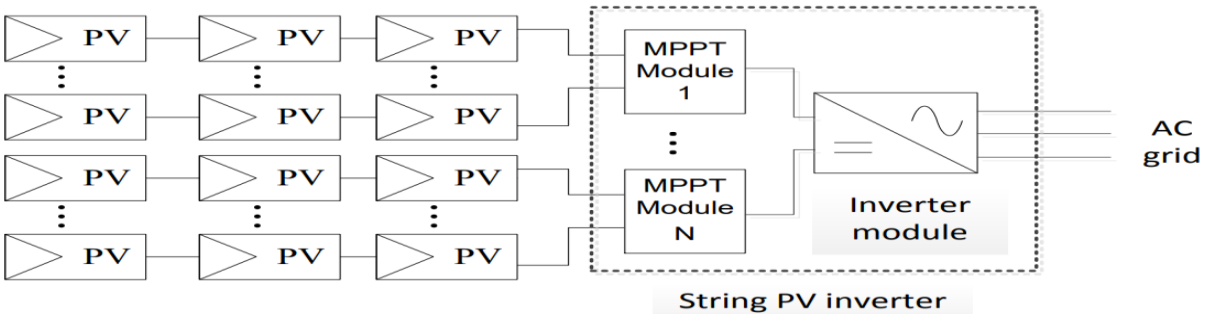

Figure 2.2 String inverters' connection in grid-tied solar plant

MPPT technology is implemented on the direct current (DC) side and is utilized for the purpose of tracking the maximum power point. The number of solar panels that can be linked to a string inverter is contingent upon the input voltage rating of the inverter [16].

The layout and simulation of the floating photovoltaic (FPV) system were conducted using PVsyst 7.4 software. This allowed for the achievement of optimal performance and the choice of equipment based on a range of variables.

CHAPTER THREE

3.1 SITE SELECTION

Baku, the capital city of Azerbaijan, is characterized by limited land availability and a high population density. The available land space could be utilized for various facilities. Floating photovoltaic (FPV) plants have emerged as a potentially optimal choice for the implementation of a 25 MW solar project in Baku.

Figure 3.1. Satellite view Boyukshor Lake, Baku [17]

Furthermore, there exist two significant documents pertaining to the city of Baku and its surrounding areas. The first is titled "The State Programme for Social and Economic Development of Baku City and its Settlements in 2014–2016," which was officially issued on January 17, 2014. The second document is a decree known as "On additional measures for improving the ecological condition, protection, and use of Boyukshor Lake," which was ratified by a Resolution of the President on December 26, 2013. This program covers reducing pollution in the lake, improving the water quality in the lake, providing a source of renewable energy, and creating jobs in the local community [18]. Therefore, the construction of FPV in Boyukshor Lake strategically and environmentally aligns with the government program.

The construction of grid-connected power energy sources is influenced by mainly two significant criteria: accessibility challenges and closeness to the power grid [19]. This factor has an impact on the expenses associated with the building of photovoltaic sources. The location is equipped with a road made of asphalt that provides access to the lake region, as depicted in Figure 3.1.

In addition, the site location is near the Boyukshor substation, facilitating the efficient and cost-effective installation of the floating photovoltaic (FPV) system onto the grid. The significant advantage of the 220/110/10 kV substation's proximity to Boyukshor Lake is illustrated in Figure 3.2. This proximity considerably mitigates power losses in the transmission line.

Figure 3.2. The view of Boyukshor substation and Boyukshor Lake [20]

The chosen location for the study is Boyukshor Lake in Baku, Azerbaijan. The lake covers an area of 16.2 km^2 and is positioned at the geographical coordinates of 40.45° N (latitude) and 49.88° E (longitude). The Boyukshor Lake is situated at an altitude of 5 meters. It is situated on the boundaries of the Binagadi, Sabunchu, and Narimanov districts inside the city of Baku.

Project summary

Geographical Site	Situation		Project settings	
Boyukshor Lake	Latitude	40.45 °N	Albedo	0.20
Azerbaijan	Longitude	49.88 °E		
	Altitude	5 m		
	Time zone	UTC+4		

Meteo data
Boyukshor Lake
PVGIS api TMY

Figure 3.3. Geographical parameters of Boyukshor Lake

CHAPTER FOUR

4.1 RESULTS AND DISCUSSION

The modeling of a 25 MW floating photovoltaic (FPV) system is conducted using PVsyst software version 7.4. The project data is displayed in Figure 3.3. Upon selecting a specific area, PVsyst software takes all relevant geographical information and meteorological data. In order to optimize operational efficiency consistently, adjustments have been made to the tilt angle and azimuth angle. The tilt and azimuth angles are determined in a manner that ensures the incident sunlight on the panels is consistently perpendicular. When the incident radiation is perpendicular to the solar PV panel, the angle of incidence will be zero, resulting in the most efficient capture of solar energy.

4.1.1 WEATHER AND SOLAR RADIATION POTENTIAL ANALYSIS

Table 4.1 displays the climatic parameters of Boyukshor Lake as acquired through the utilization of PVsyst software.

Table 4.1. Meteorological parameters of Boyukshor Lake

New simulation variant
Customised table

	GlobHor kWh/m²	GlobInc kWh/m²	DiffHor kWh/m²	BeamHor kWh/m²	T_Amb °C	WindVel m/s
January	51.6	77.2	28.52	23.1	5.63	6.5
February	50.3	59.6	37.88	12.4	5.54	6.6
March	104.7	124.9	59.05	45.6	8.22	6.1
April	159.0	175.0	67.55	91.4	12.03	6.3
May	205.2	208.1	80.82	124.4	16.93	5.5
June	212.1	204.4	76.37	135.7	22.38	5.6
July	209.0	206.5	83.83	125.1	28.63	6.2
August	200.7	215.5	66.85	133.9	28.22	6.2
September	150.5	180.7	57.77	92.7	23.59	6.3
October	86.0	110.9	47.72	38.2	17.19	5.6
November	55.9	81.0	32.82	23.0	8.02	6.6
December	38.5	55.8	25.68	12.8	9.06	6.1
Year	1523.4	1699.4	664.86	858.5	15.52	6.1

The meteorological data is obtained from the PVGIS database. The yearly average irradiation of Baku has been determined to be 1523.4 kWh/m2. Based on the data presented in Table 4.1, it can be observed that the highest recorded general temperature occurs in July

with a temperature of 28.63 ^{o}C, while the highest recorded wind speed occurs in February and November with a velocity of 6.6 m/s. An increase in temperature has a detrimental effect on the efficiency of the photovoltaic cell. In addition, higher wind velocities aid in the reduction of the PV cell's temperature, which consequently increases the cell's efficiency.

According to the GHI data, the month of December in the year 2022 exhibited the lowest monthly average of 38.5 kWh/m^2. In contrast, the month of May exhibited the highest monthly average of solar irradiance at 212.1 kWh/m^2. The GHI value is subject to fluctuations due to variations in the occurrence of rainy and dry seasons.

Diffuse Horizontal Irradiance (DHI) and Beam Horizontal Irradiance (BHI) are combined to form Global Horizontal Irradiance (GHI). The Global Tilt Irradiance (GTI), which refers to the sunlight absorbed by pv modules, is influenced by these key factors. The GTI represents the amount of energy converted into electricity by a solar module.

4.1.2 DEPLOYMENT OF SOLAR PANELS.

The photovoltaic panel deployment is constructed with fixed tilt arrays. The pv modules in fixed configurations require a predetermined tilt angle and position.

The tilt angle of an FPV can affect its annual electricity generation. Considering Boyukshor Lake's geographic location, a suggestion is put out to install solar panels with a set tilt angle of 32 degrees. The tilt angle is set to be equivalent to the latitude in order to optimize the capture of solar energy throughout the day. This position helps prevent the buildup of dust and other particles, which rain can naturally remove [21]. The entire area that the floating photovoltaic plant will cover is 142243 m^2.

The orientation of the solar panel installation has a significant impact on the power generation of the pv panel. The solar panel design is constructed in accordance with the geographic location, with a certain orientation towards the north or an azimuth angle of 0º.

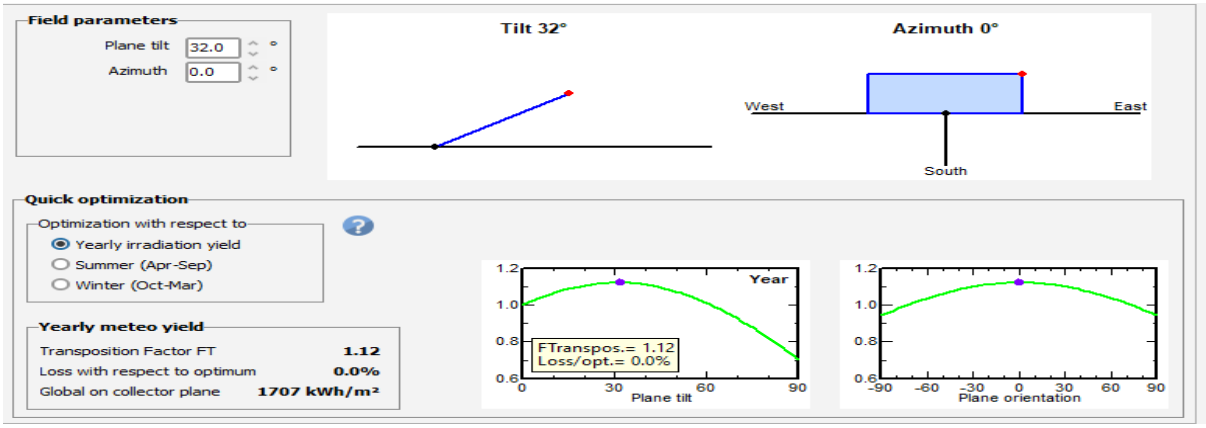

Figure 4.1. Orientation of planes

The transposition factor (TF) is an essential variable that quantifies the disparity in solar radiation received by a tilted FPV panel in comparison to a flat horizontal surface. That is the division of global irradiance on the collector plane by global horizontal irradiance (GlobHor). The preferrable value of TF is close to 1, which signifies a higher level of energy generation efficiency by the photovoltaic (PV) panel.

$$TF = \frac{Global\ irradiance\ on\ collector\ plane}{Global\ horizontal\ irradiance} \qquad (4.1)$$

Table 4.2 shows the relative loss with respect to angle tilt. As it is seen, the relative loss approaches zero in the incremental value of GTI.

Table 4.2. Simulation result of the angle tilt

Parameters	Angle Tilt		
	25°	27°	32°
GTI (kWh/m^2)	1701	1704	1707
Loss relative (%)	-0.4	-0.2	0.0

4.1.3 SINGLE LINE DIAGRAM OF FPV PLANT

The simulated solar plant utilized string inverters as its primary types of inverters. String inverters exhibit cost-effectiveness in the context of smaller systems, while also displaying an increasing level of efficiency for larger projects, alongside providing a certain degree of redundancy. The maintenance of string inverters is less complex, yet it may not achieve the same level of efficiency as central inverters in the context of large-scale applications. The selection between the two options is contingent upon the dimensions of the solar facility, objectives pertaining to efficiency, cost factors, and plans for maintenance.

The solar panel was configured in accordance with the specified design requirements. The series connection and parallel connection enhance, respectively, input voltage and current originating from the inverter.

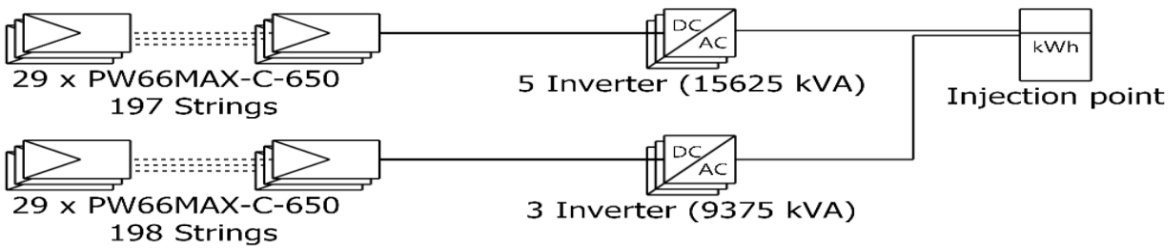

Figure 4.2. Single line diagram (SLD) of FPV plant

As seen in figure 4.3, the SLD of an FPV plant is comprised of two parts. The first section contains five arrays, and the second section contains three arrays. In the first part, one array consists of 197 strings with 29 modules in a series. Whereas, in the second part, the array consists of 198 strings with 29 modules. As we mentioned above, the voltage of one module is 32 V. All these data give us the opportunity to calculate nominal PV plant power.

$V_{array} = 29 * V_{pv} = 29 * 32 = 928$ V

$I_{pv} = P_{pv}/V_{pv} = 650 / 32$ V $= 20.3125$ A

$I_{array} = I_{pv} * n_{string} = 20.3125 * 197 = 4001.5625$ A

$P_{array} = V_{array} * I_{array} = 928 * 4001.5625 = 3713.450$ W

As 1st part consist of 5 arrays:

$P_{1st\ part} = n_{array} * P_{array} = 5 * 3713.450 = 18567.450$ W

Coming to the 2nd part:

$I_{array} = I_{pv} * n_{string} = 20.3125 * 198 = 4021.875$ A

$P_{array} = V_{array} * I_{array} = 928 * 4021.875 = 3732.300$ W

As 2nd part consist of 3 arrays:

$P_{2nd\ part} = n_{string} * P_{array} = 3 * 3732.300 = 11196.900$ W

$P_{pv\ plant} = P_{1st\ part} + P_{2nd\ part} = 18567.450 + 11196.900 = 29764.35$ W (DC)

Given that there are eight inverters, the output power of each inverter may be calculated as follows:

$P_{total\ inv} = P_{inv} * n_{inv} = 3125 * 8 = 25000$ W (AC)

$P_{nom\ ratio} = P_{pv\ plant} / P_{total\ inv} = 29764.35 / 25000 = 1.19$

There are numerous arguments for the desirability of a greater Pnom ratio. Firstly, it is imperative to check that the inverter is functioning at its optimal efficiency. When the inverter is functioning at its peak efficiency, it facilitates a higher conversion rate of direct current (DC) power into alternating current (AC) power. Consequently, this enables the photovoltaic (PV) plant to produce a greater amount of electricity.

Furthermore, an increased Pnom ratio has the potential to mitigate losses caused by clipping. Clipping losses occur when the inverter is unable to completely convert all of the direct current (DC) power generated by the solar panels into alternating current (AC) electricity. This scenario may occur when the inverter's capacity is insufficient or when the solar panels are producing an excess of electricity beyond the inverter's capacity.

Ultimately, an increased P_{nom} ratio has the potential to effectively prolong the operational longevity of the inverter. When the inverter is functioning at its peak efficiency, it produces a reduced amount of thermal energy. This practice has the potential to extend the operational durability of the inverter while simultaneously mitigating repair expenditures.

The calculation is seen below mentioned figure 4.3 that illustrates simulation results.

PV Array Characteristics

PV module		**Inverter**	
Manufacturer	Generic	Manufacturer	Generic
Model	PW66MAX-C-650	Model	SG3125-HV-20
(Original PVsyst database)		(Original PVsyst database)	
Unit Nom. Power	650 Wp	Unit Nom. Power	3125 kWac
Number of PV modules	45791 units	Number of inverters	8 units
Nominal (STC)	29.76 MWp	Total power	25000 kWac
Modules	1579 string x 29 In series	Operating voltage	875-1300 V
At operating cond. (50°C)		Max. power (=>25°C)	3593 kWac
Pmpp	27.30 MWp	Pnom ratio (DC:AC)	1.19
U mpp	986 V		
I mpp	27683 A		
Total PV power		**Total inverter power**	
Nominal (STC)	29764 kWp	Total power	25000 kWac
Total	45791 modules	Max. power	28744 kWac
Module area	142243 m²	Number of inverters	8 units
		Pnom ratio	1.19

Figure 4.3. PV array characteristics

4.1.4 DESIGN OF THE FPV

The visual representation is achieved from Helioscope software (Figure 4.4). The installation location for the FPV system must be adapted to the specific aerial conditions present at Boyukshor Lake. According to the computed area, it is determined that FPV need a minimum area measuring 400.74 meters in length and 354.95 meters in width. The maximum width of the lake is 2000 meters and coastline length is 12000 meters.

The simulated plant has 45791 solar panels. The polycrystalline module exhibits a power output of 651.7 Watt peak and a monocrystalline 650.4 Watt peak, along with 8 inverters with a capacity of 3125 kilowatts (kW) each. The system layout comprises a series connection of 29 solar panels, with each array consisting of 197 and 198 parallel solar panels, respectively, to the first and second parts of the system. This arrangement results in a total of 1579 strings.

Figure 4.4. The view of FPV plant on the Boyukshor Lake.

4.1.5 COMPARATIVE SIMULATION RESULTS OF PERFORMANCE RATIO AND EFFICIENCY

The monocrystalline FPV plant generates a yearly energy output of 44189.702 MWh, while the FPV with polycrystalline modules generates a yearly energy output of 45060.04 MWh. The precise amount of energy transmitted into the grid is determined after taking into account losses in both the inverter and the photovoltaic panel. The normalized energy yield and performance ratio (PR) are significant performance indicators.

The computed value for the Lc-collection loss, which represents the loss in solar panel efficiency, is found to be 0.54 kWh/kWp/day for monocrystalline FPV systems and 0.46 kWh/kWp/day for polycrystalline FPV systems. Since the inverters used in "Case 1" and "Case 2" simulations were the same, the system loss (Ls) for both monocrystalline and polycrystalline FPV was found to be 0.05 kWh/kWp/day (Figures 4.5 and 4.6). The mean value of the produced useful energy, denoted as Y_f, is determined to be 4.07 and 4.05 kWh/kWp/day, respectively, with monocrystalline and polycrystalline FPV plants.

The performance ratio (PR) is expressed as a percentage and is determined by dividing the actual generation of the plant by the plant's generation in an ideal scenario.

$$PR = \frac{Actual\ output}{Output\ under\ ideal\ case} = \frac{Yf}{Yr} = \frac{E\_Grid}{GlobInc * PnomArray} \quad (4.2)$$

Table 4.3. Produced useful energy for monocrystalline and polycrystalline FPV.

	E_Grid (poly)(kWh)	E_Grid (mono)(kWh)
January	2176578	2133858
February	1666696	1635463
March	3452302	3385308
April	4727626	4636216
May	5524325	5416638
June	5303299	5204076
July	5252423	5150772
August	5461726	5355489
September	4691289	4598304
October	2985842	2928329
November	2266501	2222973
December	1551399	1522277
Year	45060004	44189702

GlobInc = 1699.4 kWh/m^2 (Table 4.1)

PnomArray= 29764 kWp (Figure 4.4)

PR_{mono} = 44189702 / (1699.4 * 29764) = 0.8736 ≈ 0.874 (Figure 4.5)

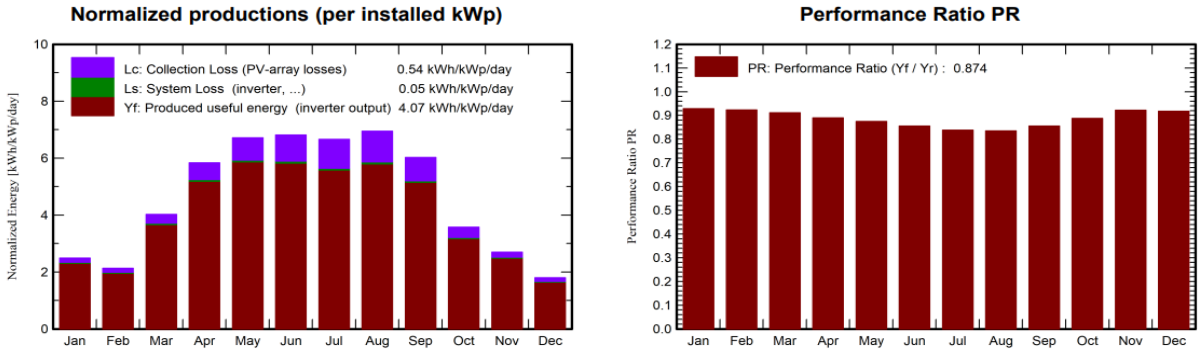

Figure 4.5. The normalized energy yield and performance ratio of monocrystalline FPV plant

PR_{poly} = 45060004 / (1699.4 * 29764) = 0.8908 ≈ 0.891 (Figure 4.6)

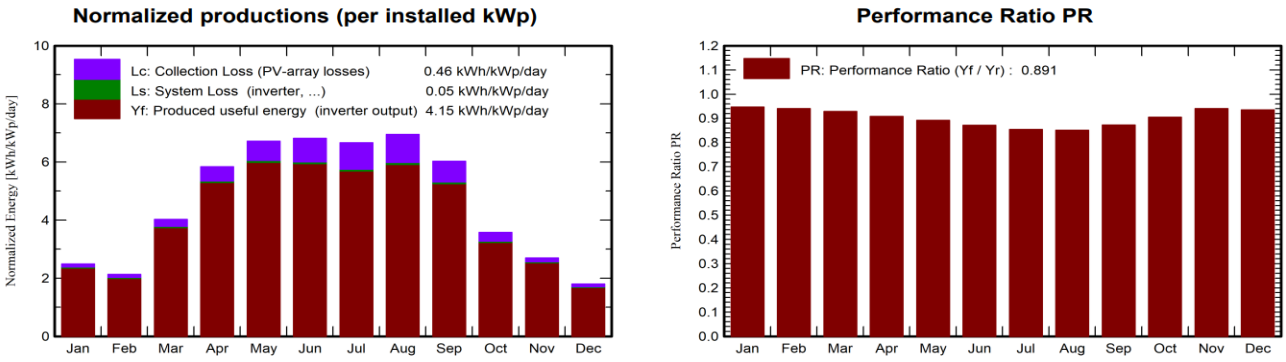

Figure 4.6. The normalized energy yield and performance ratio of polycrystalline FPV plant

As it is seen from figure 4.8 and 4.9 polycrystalline FPV plants' PR is higher than the monocrystalline FPV plant. Under specific circumstances, it has been shown that the performance ratio of polycrystalline photovoltaic (PV) plants tends to surpass that of monocrystalline PV plants. The primary factor contributing to this discrepancy is the variation in their respective manufacturing procedures and the subsequent characteristics of the materials produced.

The presence of grain boundaries and defects in polycrystalline silicon results in the development of energy levels within the material, which have the potential to capture electrons and therefore hinder their mobility. Nevertheless, these imperfections also give rise to extra channels for the absorption of light, boosting the overall efficiency of converting light into electricity, particularly in situations with limited light intensity.

In general, it can be inferred that in situations characterized by limited illumination, the utilization of polycrystalline silicon serves to counteract the diminished electron mobility by augmenting light absorption, hence leading to an elevated performance ratio [22].

In order to simulate floating solar systems using PVsyst, certain adjustments need to be made to the PV panel configuration parameters, as the software primarily supports ground-mounted solar systems. The primary distinction between floating photovoltaic (FPV) and solar photovoltaic (SPV) systems is the change in cell temperature. Consequently, modifications have been implemented to alter the thermal loss factor. The thermal loss factor (U_C) for floating photovoltaic (FPV) systems is designated as 25 W/m^{2}K, whereas for solar photovoltaic (SPV) systems, it is designated as 20 W/m^{2}K (Figure 4.7).

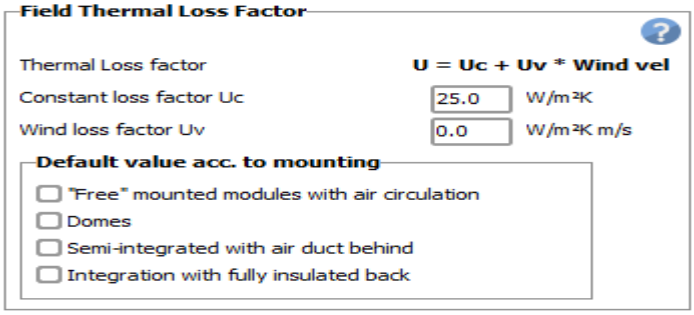

Figure 4.7. Detailed losses configuration parameters in PVsyst

The Sankey diagram is a comprehensive representation of energy losses, encompassing factors such as temperature, mismatch, and ohmic losses. Figure 4.8 illustrates all the losses in the monocrystalline and polycrystalline FPVs. Following the photovoltaic (PV) conversion process and accounting for associated losses, the energy output of the FPV system amounts to 44725449 kilowatt-hours (kWh) and 45603692 kWh, respectively, for monocrystalline and polycrystalline FPV. The various losses are attributed to fluctuations in ambient temperature and solar radiation levels, mismatch losses in the connection of photovoltaic (PV) panels, and losses caused by wiring. The AC power transmitted to the grid is 44189702 kWh and 45060004 kWh, respectively, for monocrystalline and polycrystalline FPV.

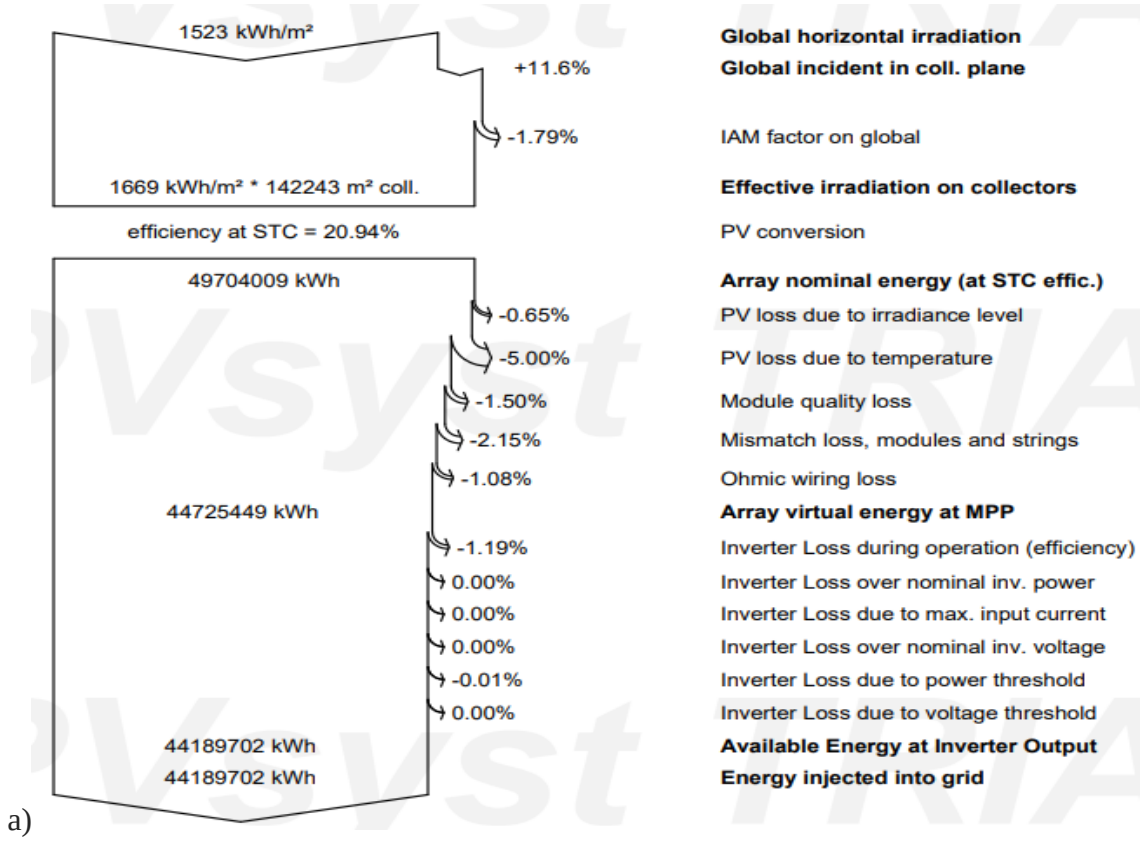

a)

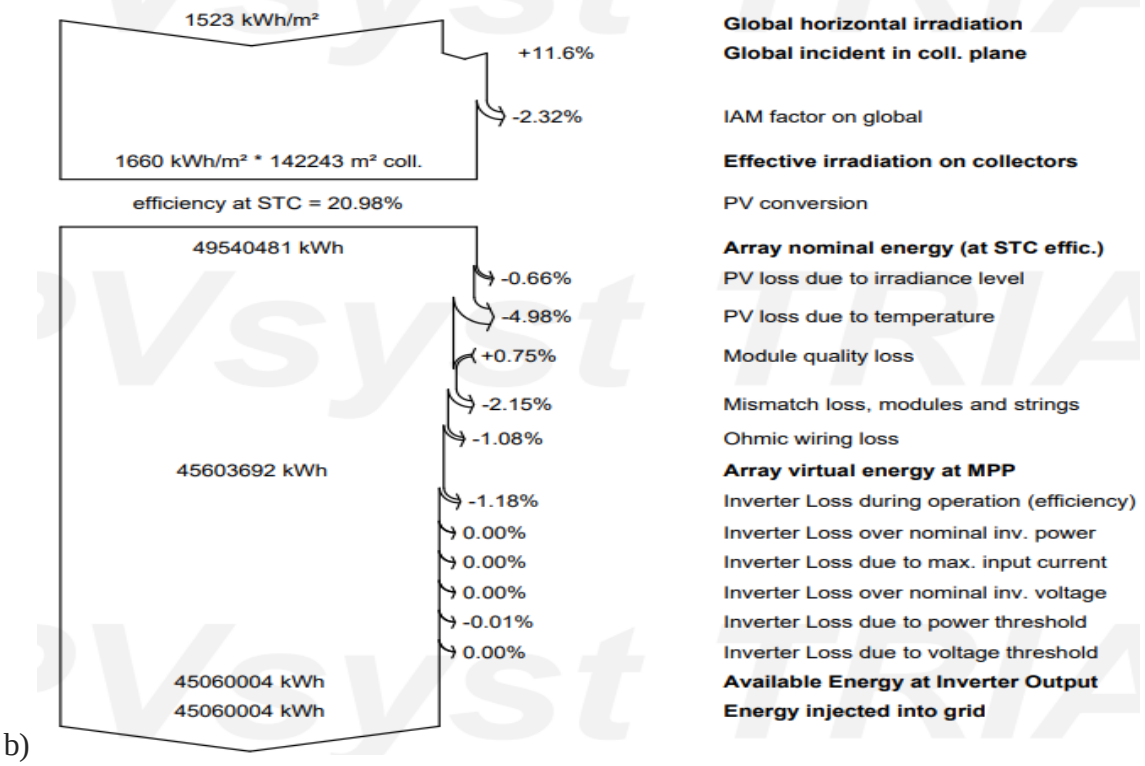

b)

Figure 4.8. Loss diagram of a) Monocrystalline FPV b) Polycrystalline FPV

The efficiency of a photovoltaic (PV) plant is a metric that can be measured to assess its ability to convert solar energy into electrical power. This metric is commonly represented as a percentage, with higher values referring to superior efficiency. The typical efficiency range for FPV plants spans from 15% to 22%, contingent upon the specific solar panel technology employed and the overall configuration of the FPV plant. As it is seen from figure 4.9, the system efficiency of monocrystalline FPV and polycrystalline FPV is, respectively, 20.94% and 20.98%.

CF evaluates the efficiency with which a power plant employs its installed capacity during a designated time period, taking into account the plant's operational availability. The calculation involves dividing the actual energy production by the potential energy production, under the assumption that the facility operated at its installed capacity throughout the entire period and encountered no maintenance or other factors that could cause downtime.

$$CF = \frac{Actual\ output}{8760\ hours * Installed\ capacity} \quad (4.3)$$

$$CF_{mono} = \frac{44189702}{8760 * 29744} * 100\% = 16.9\%$$

$$CF_{poly} = \frac{45060004}{8760 * 29744} * 100\% = 17.2\%$$

The evaluation of the FPV design's performance can be determined by three key parameters: system efficiency, capacity factor (CF), and performance ratio (PR). The optimization results indicate that the system's efficiency (η), capacity factor (CF), and performance ratio (PR) are determined to be 20.94%, 16.9%, and 87.4% for monocrystalline FPV, 20.98%, 17.2%, and 89.1% for polycrystalline FPV, respectively.

CHAPTER FIVE

ECONOMIC EVALUATION AND ENVIRONMENTAL IMPACT

5.1. ECONOMIC EVALUATION

The comprehensive project cost estimation encompasses CAPEX (expenditures on solar panels, floating structures, inverters, studies, insurance, taxes, and installation) and OPEX (expenditures on operation and maintenance). Monocrystalline FPV expenditure details are in Tables 5.1 and 5.2, while polycrystalline FPV costs are listed in Tables 5.3 and 5.4. The compared system summary both for a 25 MW monocrystalline and polycrystalline plant is shown in table 5.5.

Table 5.1. CAPEX of monocrystalline FPV plant

Cost of the system

Installation costs

Item	Quantity units	Cost AZN	Total AZN
PV modules			
ZXM8-TPLDD-132-650	45791	500.00	22,895,500.00
Supports for modules	45791	40.00	1,831,640.00
Inverters			
SG3125-HV-20	8	340,000.00	2,720,000.00
Other components			
Accessories, fasteners	1	850,000.00	850,000.00
Wiring	1	1,700,000.00	1,700,000.00
Combiner box	1579	1,000.00	1,579,000.00
Monitoring system, display screen	1	510,000.00	510,000.00
Measurement system, pyranometer	1	510,000.00	510,000.00
Surge arrester	1	510,000.00	510,000.00
Studies and analysis			
Engineering	1	1,700,000.00	1,700,000.00
Permitting and other admin. Fees	1	850,000.00	850,000.00
Environmental studies	1	510,000.00	510,000.00
Economic analysis	1	510,000.00	510,000.00
Installation			
Global installation cost per module	45791	165.75	7,589,858.25
Global installation cost per inverter	8	800,000.00	6,400,000.00
Transport	1	1,500,000.00	1,500,000.00
Settings	1	3,000,000.00	3,000,000.00
Grid connection	1	3,400,000.00	3,400,000.00
Insurance			
Building insurance	1	170,000.00	170,000.00
Transport insurance	1	850,000.00	850,000.00
Liability insurance	1	170,000.00	170,000.00
Delay in start-up insurance	1	850,000.00	850,000.00
Land costs			
Land purchase	142243	250.00	35,560,750.00
Land preparation	1	3,000,000.00	3,000,000.00
Land taxes	1	0.00	3,556,075.00
Taxes			
VAT	1	0.00	280,000.00
Local taxes	1	0.00	150,000.00
		Total	103,152,823.25
		Depreciable asset	28,297,140.00

Table 5.2. OPEX of monocrystalline FPV plant

Cost of the system

Operating costs

Item	Total AZN/year
Maintenance	
Provision for inverter replacement	544,000.00
Salaries	500,000.00
Repairs	150,000.00
Cleaning	70,000.00
Security fund	60,000.00
Insurance	
Facilities insurance	150,000.00
Liability insurance	130,000.00
Business interruption insurance	70,000.00
Lack of sunlight insurance	65,000.00
Administrative, accounting	300,000.00
Taxes	
Local taxes	100,000.00
Property taxes	50,000.00
Other taxes	40,000.00
Total (OPEX)	2,229,000.00

Table 5.3. CAPEX of polycrystalline FPV plant

Cost of the system

Installation costs

Item	Quantity units	Cost AZN	Total AZN
PV modules			
PW66MAX-C-650	45791	460.00	21,063,860.00
Supports for modules	45791	40.00	1,831,640.00
Inverters			
SG3125-HV-20	8	340,000.00	2,720,000.00
Other components			
Accessories, fasteners	1	850,000.00	850,000.00
Wiring	1	1,700,000.00	1,700,000.00
Combiner box	1579	1,000.00	1,579,000.00
Monitoring system, display screen	1	510,000.00	510,000.00
Measurement system, pyranometer	1	510,000.00	510,000.00
Surge arrester	1	510,000.00	510,000.00
Studies and analysis			
Engineering	1	1,700,000.00	1,700,000.00
Permitting and other admin. Fees	1	850,000.00	850,000.00
Environmental studies	1	510,000.00	510,000.00
Economic analysis	1	510,000.00	510,000.00
Installation			
Global installation cost per module	45791	165.75	7,589,858.25
Global installation cost per inverter	8	800,000.00	6,400,000.00
Transport	1	1,500,000.00	1,500,000.00
Settings	1	3,000,000.00	3,000,000.00
Grid connection	1	3,400,000.00	3,400,000.00
Insurance			
Building insurance	1	170,000.00	170,000.00
Transport insurance	1	850,000.00	850,000.00
Liability insurance	1	170,000.00	170,000.00
Delay in start-up insurance	1	850,000.00	850,000.00
Land costs			
Land purchase	142243	250.00	35,560,750.00
Land preparation	1	3,000,000.00	3,000,000.00
Land taxes	1	0.00	3,556,075.00
Taxes			
VAT	1	0.00	280,000.00
Local taxes	1	0.00	150,000.00
		Total	101,321,183.25
		Depreciable asset	26,465,500.00

Table 5.4. OPEX of polycrystalline FPV plant

Cost of the system

Operating costs

Item	Total AZN/year
Maintenance	
Provision for inverter replacement	544,000.00
Salaries	500,000.00
Repairs	150,000.00
Cleaning	70,000.00
Security fund	60,000.00
Insurance	
Facilities insurance	150,000.00
Liability insurance	130,000.00
Business interruption insurance	70,000.00
Lack of sunlight insurance	65,000.00
Bank charges	65,000.00
Administrative, accounting	300,000.00
Taxes	
Local taxes	100,000.00
Property taxes	50,000.00
Other taxes	40,000.00
Total (OPEX)	2,294,000.00

Table 5.5. Compared system summary for monocrystalline and polycrystalline FPV

	Monocrystalline FPV plant	Polycrystalline FPV plant
Total installation cost	103,152,823.25 AZN	101,321,183.25 AZN
Operating costs	2,940,928.80 AZN/year	3,026,689.39 AZN/year
Produced Energy	44190 MWh/year	45060 MWh/year
Cost of produced energy (LCOE)	0.1500 AZN/kWh	0.1477 AZN/kWh
Payback period	7.3 years	7 years

Given the 20-year guaranteed electricity sale price of 0.38 AZN, as stipulated in the tariff warranty, the proposal is formally submitted for consideration. Considering expenditures and electricity sale prices the return on investment is computed (Table 5.6)

Table 5.6. Compared return on investment values for monocrystalline FPV and polycrystalline FPV.

	Monocrystalline FPV plant	Polycrystalline FPV plant
Payback period	7.3 years	7 years
Net present value (NPV)	316,114,669.04 AZN	325,837,776.32 AZN
Internal rate of return (IRR)	12.94 %	13.48 %
Return on investment (ROI)	306.5 %	321.6 %

Table 5.6 demonstrates that the 25 MW polycrystalline FPV plant exhibits a shorter payback period of 7 years compared to the 7.3 years of the monocrystalline FPV plant. Furthermore, the polycrystalline FPV plant boasts a significantly higher NPV of 325,837,776.32 AZN, surpassing the monocrystalline FPV plant's NPV of 316,114,669.04 AZN. Consequently, considering both the payback period and NPV, the 25 MW polycrystalline FPV plant emerges as the more economically advantageous option.

5.2. ENVIRONMENTAL IMPACT

The carbon footprint refers to the comprehensive quantity of greenhouse gases (GHGs) generated as a result of human activities, encompassing both direct and indirect emissions. The standard unit of measurement is typically metric tons of carbon dioxide (CO2) equivalents. The carbon footprint refers to the total amount of carbon dioxide (CO2) emissions generated by various activities throughout a specific time period, often one year.

Installation of solar panels will result in a decrease in carbon dioxide (CO2) emissions. The primary environmental advantages and impacts of FPV power plants are the carbon dioxide emissions they reduce when compared to conventional power plants during

electricity generation. Quantifying these savings is possible using the generic equation provided below [23].

$$GHG_{savings} = \sum_{y=1}^{n} GHG_{reference,y} - GHG_{project,y} \quad (5.1)$$

The variable $GHG_{savings}$ represents the amount of greenhouse gas emissions that are prevented as a result of generating energy from renewable sources over a specific time period, denoted as n, measured in metric tons of carbon dioxide equivalent (tCO_2e). The $GHG_{reference,\ y}$ reflects the annual greenhouse gas emissions linked to the production of an equivalent quantity of energy using reference technology. It is measured in metric tons of carbon dioxide equivalent per year (tCO2e/year). The $GHG_{project}$ refers to the annual greenhouse gas emissions resulting from renewable energy production, measured in metric tons of carbon dioxide equivalent (tCO2e). The variable n represents the last year of operation for the project.

The computation of the $GHG_{reference}$ and $GHG_{project}$ will vary in complexity based on the output and the renewable energy source utilized for generating. The reference scenario would represent the equivalent reduction in fossil fuel emissions as a result of switching to renewable energy sources. Simulation results in Figure 5.1 illustrate the projected carbon emissions for the next 25 years. The analysis reveals that the installation of the monocrystalline FPV system would save around 437,986.1 tons of CO_2 emissions, whereas the polycrystalline FPV system would save around 447,480.1 tons. The diagram provides evidence of the viability of the FPV system. Opting for a polycrystalline FPV rather than a monocrystalline FPV will effectively mitigate additional carbon emissions.

a)

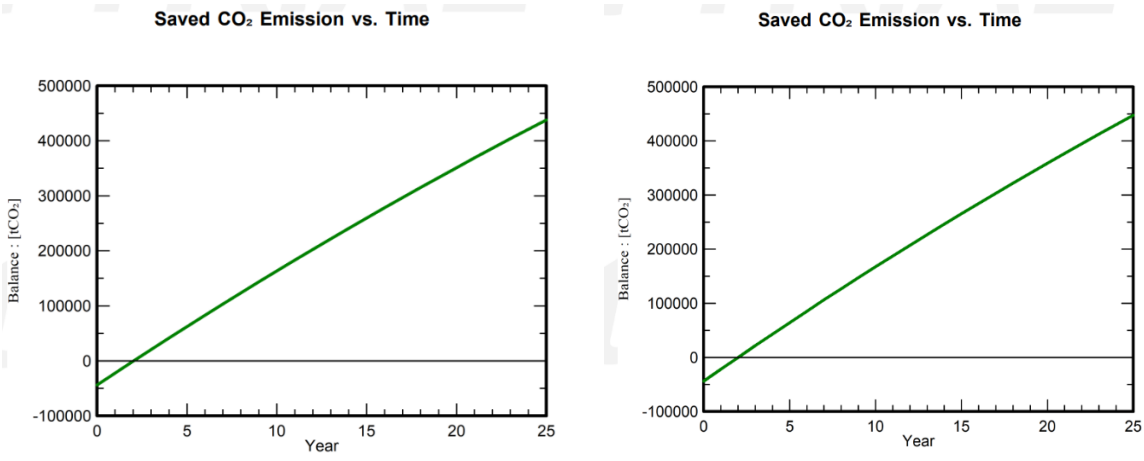

Figure 5.1. Carbon emissions for the system in the next 25 years. a) Monocrystalline FPV and b) Polycrystalline FPV

CHAPTER SIX

6.1 CASE 3 ANALYSIS

Analysis showed that case 2 is more efficient than the case 1. Therefore case 3 will combine Sepsa inverter (100 kW, 450-820 V) with the polycrystalline module.

Figure 6.1 illustrates the monthly normalized energy production, encompassing both the array and system losses. The occurrence of both losses is reduced in the winter and increases in the summer. The array experiences a significant increase in losses during the summer months as a result of reduced efficiency caused by high temperatures. The collection loss, L_C, is determined to be 0.46 $kWh/kW_p/day$, while the system loss, L_S, is 0.12 $kWh/kW_p/day$. The Y_f (produced useful energy) is 4.07 $kWh/kW_p/day$.

Additionally, right hand side diagram in Figure 6.1 illustrates the monthly performance ratios. The PR represents the ultimate efficiency of the PV system. The mean annual PR is determined to be 0.874.

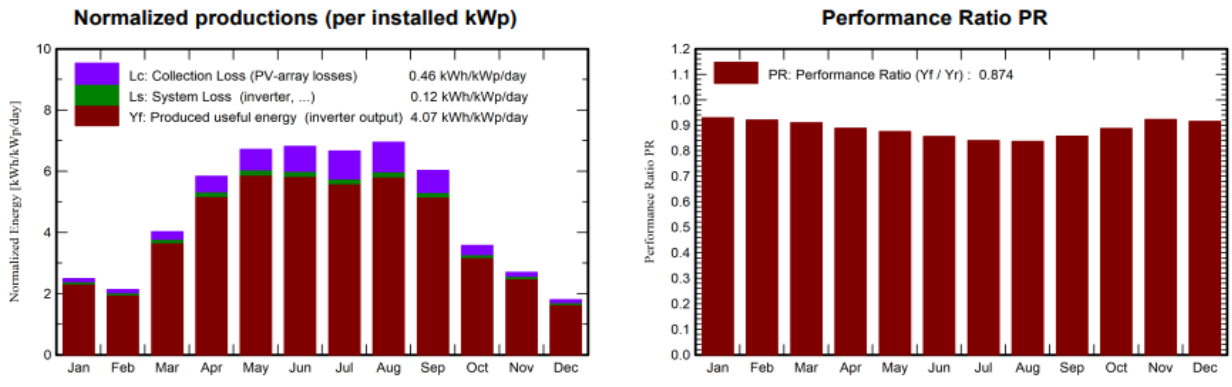

Figure 6.1. Normalized production and performance ratio of case 3

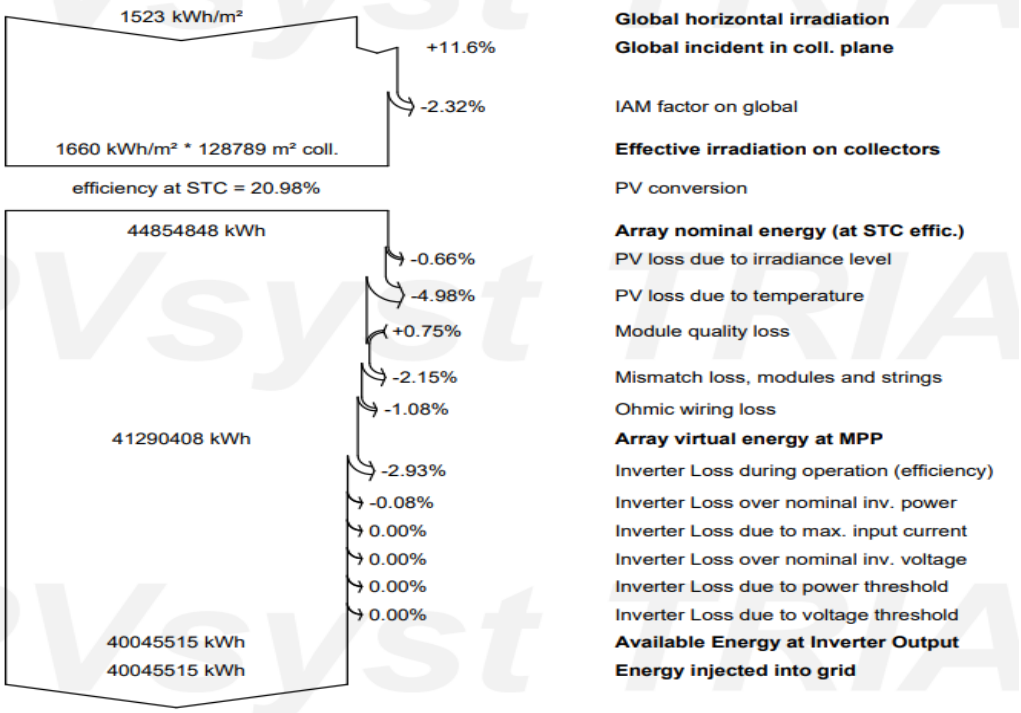

Figure 6.2. Loss diagram of case 3

The analysis of the losses incurred by the solar power facility is presented in Figure 6.2 The estimate of electricity injected to the grid includes the computation of optical losses, array losses, and system losses. When losses are disregarded, an energy output of 44854,848 MWh is achieved. An average yearly generation of 40045,515 MWh is achieved despite the occurrence of losses.

Capacity factor is calculated below:

$$CF_{3rd\ case} = \frac{40045518}{8760 * 26949} * 100\% = 17\%$$

Table 6.1 CAPEX of case 3

Cost of the system

Installation costs

Item	Quantity units	Cost AZN	Total AZN
PV modules			
PW66MAX-C-650	41460	460.00	19,071,600.00
Supports for modules	41460	40.00	1,658,400.00
Inverters			
Sepsa Solar 100 mod-ID	250	30,000.00	7,500,000.00
Other components			
Accessories, fasteners	1	700,000.00	700,000.00
Wiring	1	1,400,000.00	1,400,000.00
Combiner box	2073	500.00	1,036,500.00
Monitoring system, display screen	1	300,000.00	300,000.00
Measurement system, pyranometer	1	500,000.00	500,000.00
Surge arrester	1	400,000.00	400,000.00
Studies and analysis			
Engineering	1	1,700,000.00	1,700,000.00
Permitting and other admin. Fees	1	850,000.00	850,000.00
Environmental studies	1	450,000.00	450,000.00
Economic analysis	1	500,000.00	500,000.00
Installation			
Global installation cost per module	41460	140.00	5,804,400.00
Global installation cost per inverter	250	10,000.00	2,500,000.00
Transport	1	2,000,000.00	2,000,000.00
Settings	1	3,000,000.00	3,000,000.00
Grid connection	1	3,400,000.00	3,400,000.00
Insurance			
Building insurance	1	170,000.00	170,000.00
Transport insurance	1	800,000.00	800,000.00
Liability insurance	1	150,000.00	150,000.00
Delay in start-up insurance	1	830,000.00	830,000.00
Land costs			
Land purchase	128789	250.00	32,197,250.00
Land preparation	1	2,500,000.00	2,500,000.00
		Total	89,418,150.00

In order to execute the suggested 25MW floating PV system in Boyukshor Lake, it is important to possess a well-defined understanding of the implementation expenses. We have computed the estimated expense in AZN in this analysis. The necessary components for this project include PV modules, inverters, combiner boxes, floating pontoon, surge arrestors, lightning rod, wiring, and so on.

The estimated lifespan of our suggested PV system is 35 years. The CAPEX and OPEX expenditures are detailly shown in table 6.1 and 6.2. The capital expenditures (CAPEX) amount to 89,418,150 AZN whereas the operating expenses (OPEX) are 3,245,000 AZN. Return of investment data shown in table.

Table 6.2. OPEX of Case 3

Cost of the system

Operating costs

Item	Total AZN/year
Maintenance	
Provision for inverter replacement	1,500,000.00
Salaries	500,000.00
Repairs	150,000.00
Cleaning	70,000.00
Security fund	60,000.00
Insurance	
Facilities insurance	150,000.00
Liability insurance	130,000.00
Business interruption insurance	70,000.00
Lack of sunlight insurance	60,000.00
Bank charges	65,000.00
Administrative, accounting	300,000.00
Taxes	
Local taxes	100,000.00
Property taxes	50,000.00
Other taxes	40,000.00
Total (OPEX)	3,245,000.00

Table 6.3. Return on investment summary of case 3

	Case 3
Payback period	7.8 years
Net present value (NPV)	237,379,269.76
Internal rate of return (IRR)	11.89 %
Return on investment (ROI)	265.5 %

The designed FPV will generate approximately 40045.518 MWh annually over the course of the 35-year project life. The estimation of Lifecycle Carbon Emissions (LCE) from various electricity production sources is conducted. The lifetime usable electricity generated from rooftop solar PV is estimated to emit approximately 386956.9 tCO2 the lifecycle carbon emission is shown in figure 6.3.

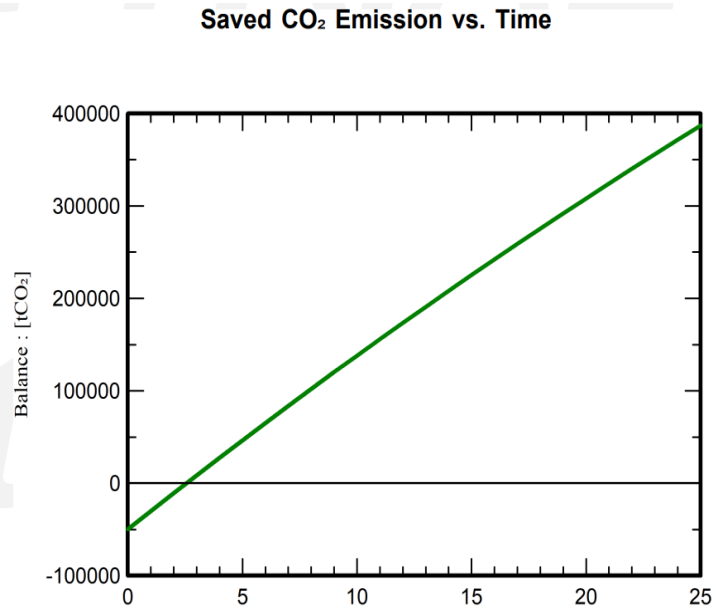

Figure 6.3. Lifecycle carbon emission of case 3

CHAPTER SEVEN

7. 1 CONCLUSION

The notion of a floating PV power plant is a modern and efficient way to boost grid electrical power generation without the need for additional land. This study presents a comprehensive analysis of a 25 MW floating solar PV system project in Boyukshor Lake, Baku.

The design of the FPV system in the Boyukshor Lake is capable of meeting the feasibility criteria. Over a span of 1 year, the average yearly amount of global horizontal irradiance (GHI) potential is 1523.4 kilowatt-hours per square meter per day. This is accompanied by an average wind speed of 6.1 meters per second and an air temperature of 15.52 degrees Celsius. The FPV plant benefits from excellent road accessibility and proximity to the electricity grid.

The power plant comprises five primary components. Case one and two employ an identical quantity of 45,791 solar modules. The solar panels are organized 29 solar panels in a series and 197-198 strings of solar panels. The FPV is designed with a 1579 DC combiner box and 8 Sungrow inverters, each with a capacity of 3125 kW. Case 3 employs a total of 41460 solar modules. The photovoltaic plant is organized into 20 strings, and every string is comprised of 20 PV modules in a series. The FPV design incorporates a 2073 DC combiner box and a 250 Pepsa inverter with a capacity of 100 kW.

The below mentioned table 7.1 comparably shows PR, CF, efficiency, installation cost, LCE and payback period values of all three cases.

Table 7.1. Comparative values of simulated parameters in all 3 cases

	PR	Efficiency	CF	Install. cost	LCE	Payback period
Case 1	87.4%	20.94%	16.9%	103,152,823.25AZN	437,986.1 tCO_2	7.3 years
Case 2	89.1%	20.98%	17.1%	101,321,183.25AZN	447,480.2 tCO_2	7 years
Case 3	87.4%	20.98%	17%	89,418,150	386,956.9 tCO_2	7.8 years

Summarizing all these three cases we can say that case two is more profitable and more efficient than 1st and 2nd cases.

The implementation of a FPV plant in Boyukshor Lake is an excellent concept for harnessing solar energy. This approach effectively decreases environmental pollution, mitigates land shortages, and fulfills Azerbaijan's growing energy needs.

7.2 FUTURE WORKS

To optimize a floating PV plant design, it is recommended to evaluate the technological viability of using either single-axis or dual-axis solar trackers. Take into account variables such as water flow, wind forces, and extra maintenance requirements. In addition, utilizing modeling and simulation techniques to quantify the enhanced energy output achieved by the implementation of trackers at Boyukshor Lake. This analysis should take into account the unique solar irradiation patterns and seasonal fluctuations.

Furthermore, find the most suitable battery storage capacity by considering aspects such as required power reserves, peak power smoothing, and involvement in grid support services.

Examine several battery technologies, such as lithium-ion and flow batteries, in order to choose the most appropriate choice for your specific application.

REFERENCE

1. Shema, S. S., Daut, I., Irwanto, M., Shatri, C., Syafawati, N., & Ashbahani, N. (2011, June). Study of inverter design and topologies for photovoltaic system. In *International Conference on Electrical, Control and Computer Engineering 2011 (InECCE)* (pp. 501-504). IEEE.
2. Albadi, M. H., Al Abri, R. S., Masoud, M. I., Al Saidi, K. H., Al Busaidi, A. S., Al Lawati, A., ... & Al Farsi, I. (2014). Design of a 50 kW solar PV rooftop system. *International Journal of Smart Grid and Clean Energy*, *3*(4), 402_409.
3. Kumar, B. S., & Sudhakar, K. (2015). Performance evaluation of 10 MW grid connected solar photovoltaic power plant in India. *Energy reports*, *1*, 184-192.
4. Muscat, M. (2014). *A study of floating PV module efficiency* (Master's thesis, University of Malta).
5. Cazzaniga, R., Cicu, M., Rosa-Clot, M., Rosa-Clot, P., Tina, G. M., & Ventura, C. (2018). Floating photovoltaic plants: Performance analysis and design solutions. *Renewable and Sustainable Energy Reviews*, *81*, 1730-1741.
6. Luo, W., Isukapalli, S. N., Vinayagam, L., Ting, S. A., Pravettoni, M., Reindl, T., & Kumar, A. (2021). Performance loss rates of floating photovoltaic installations in the tropics. *Solar Energy*, *219*, 58-64.
7. Kim, S. M., Oh, M., & Park, H. D. (2019). Analysis and prioritization of the floating photovoltaic system potential for reservoirs in Korea. *Applied Sciences*, *9*(3), 395.
8. Rahman, M. W., Mahmud, M. S., Ahmed, R., Rahman, M. S., & Arif, M. Z. (2017, April). Solar lanes and floating solar PV: New possibilities for source of energy generation in Bangladesh. In *2017 Innovations in Power and Advanced Computing Technologies (i-PACT)* (pp. 1-6). IEEE.
9. Sahu, A., Yadav, N., & Sudhakar, K. (2016). Floating photovoltaic power plant: A review. *Renewable and sustainable energy reviews*, *66*, 815-824
10. Agrawal, M., Chhajed, P., & Chowdhury, A. (2022). Performance analysis of photovoltaic module with reflector: Optimizing orientation with different tilt scenarios. *Renewable Energy*, *186*, 10-25.
11. *Solar Radiation on a Tilted Surface | PVEducation*. (n.d.). https://www.pveducation.org/pvcdrom/properties-of-sunlight/solar-radiation-on-a-tilted-surface
12. A. (2021, February 1). *Solar panel temperature*. Solar Calculator. https://solarcalculator.com.au/solar-panel-temperature/#:~:text=Solar%20panel%20temperature%20coefficient&text=Most%20panels%20have%20a%20temperature,have%20a%20higher%20temperate%20tolerance.
13. Ali, H., & Khan, H. A. (2023, October). Comparative Analysis of Solar Photovoltaic Module Technologies in Diverse Environmental Conditions in Pakistan. In *2023 IEEE Global Humanitarian Technology Conference (GHTC)* (pp. 55-61). IEEE.
14. Achour, Y., Berrada, A., Arechkik, A., & El Mrabet, R. (2023). Techno-Economic Assessment of hydrogen production from three different solar photovoltaic technologies. *International Journal of Hydrogen Energy*.
15. Jude, T. (2023, December 3). *Monocrystalline vs. Polycrystalline Solar Panels: 2023 Guide*. MarketWatch. https://www.marketwatch.com/guides/solar/monocrystalline-vs-polycrystalline-solar-panels/

16. Gagrica, O., Nguyen, P. H., Kling, W. L., & Uhl, T. (2015). Microinverter curtailment strategy for increasing photovoltaic penetration in low-voltage networks. *IEEE Transactions on Sustainable Energy*, *6*(2), 369-379.
17. *Boyukshor Lake*. (n.d.). Google Earth. Retrieved December 26, 2023, from https://earth.google.com/web/@40.45143795,49.88240674,10.93801948a,7077.06234849d,35y,0.00000055h,0t,0r/data=OgMKATA.
18. *Rehabilitation Project of Absheron Lakes - Clean City*. (n.d.). https://tamizshahar.az/en/projects/4
19. Yousuf, H., Khokhar, M. Q., Zahid, M. A., Kim, J., Kim, Y., Cho, E. C., ... & Yi, J. (2020). A review on floating photovoltaic technology (FPVT). *Current Photovoltaic Research*, *8*(3), 67-78.
20. *President, First Lady inaugurate new substation in Boyukshor [UPDATE]*. (2020, July 16). Azernews.Az. https://www.azernews.az/nation/167074.html
21. "Intrenational Journal of software engg. and its applications",Vol.8,No.1,pp.75-84,2014.
22. Abdel-Khalek, H., Shalaan, E., Abd-El Salam, M., & El-Mahalawy, A. M. (2018). Effect of illumination intensity on the characteristics of Cu (acac) 2/n-Si photodiode. *Synthetic Metals*, *245*, 223-236.
23. Lu, M., & Lai, J. (2020). Review on carbon emissions of commercial buildings. *Renewable and Sustainable Energy Reviews*, *119*, 109545.